JACS
JOURNAL OF THE AMERICAN CHEMICAL SOCIETY
Communication
pubs.acs.org/JACS

On/Off Photoswitching in a Cyanide-Bridged $\{Fe_2Co_2\}$ Magnetic Molecular Square

Abhishake Mondal,[†] Yanling Li,[†] Mannan Seuleiman,[†] Miguel Julve,[‡] Loïc Toupet,[§] Marylise Buron-Le Cointe,*[,§] and Rodrigue Lescouëzec*[,†]

[†]Institut Parisien de Chimie Moléculaire (IPCM), UMR 7201, UPMC Paris 6, 4 place Jussieu, 75252 Paris cedex 5, France

[‡]Instituto de Ciencia Molecular (ICMol), Facultat de Química, Universitat de València, C/Catedrático José Beltrán 2, 46980 Paterna, València, Spain

[§]Institut de Physique de Rennes, Université Rennes 1-CNRS, UMR 6251, Bat 11A Campus de Beaulieu, 35042 Rennes Cedex, France

Supporting Information

ABSTRACT: A repeatable bidirectional paramagnetic ↔ diamagnetic photomagnetic effect has been observed in the cyanide-bridged Fe−Co square complex $\{[Fe\{B(pz)_4\}(CN)_3]_2[Co(bik)_2]_2\}(ClO_4)_2\cdot 3H_2O$ [$B(pz)_4$ = tetrapyrazolylborate, bik = bis(1-methylimidazol-2-yl)ketone]. Magnetic measurements and low-temperature single-crystal X-ray diffraction experiments have shown that a complete electron transfer from the diamagnetic Fe^{II} −Co^{III} state to the paramagnetic Fe^{III} −Co^{II} metastable state is induced by 808 nm laser light irradiation, whereas the diamagnetic state is recovered in an almost quantitative yield under irradiation at 532 nm.

The design of switchable molecular materials has become an important topic in the field of materials science, offering rich potential applications for future molecular electronic devices.[1] For example, molecules exhibiting on/off switching of their magnetization appear to be good candidates for information storage on the molecular scale. Reproducible control of the magnetic properties at a given temperature via light irradiation (as opposed to thermal stimulus) turns out to be an important issue in such a perspective. Cyanide-based chemistry has provided many molecular switches,[2] among which the Fe−Co Prussian Blue analogues (PBAs) are probably the most emblematic examples of photomagnetic materials. In these inorganic polymers, visible-light irradiation can induce electron transfer (ET) from Fe^{II}_{LS} to Co^{III}_{LS} (LS = low-spin), which is accompanied by a change of the spin state of the Co center. Thus, the diamagnetic (dia) Fe^{II}_{LS}−Co^{III}_{LS} pairs are converted into metastable paramagnetic (para) Fe^{III}_{LS}−Co^{II}_{HS} pairs (HS = high-spin), and a diamagnetic PBA can be subsequently transformed into a ferrimagnet.[3] The diamagnetic ground state can then be recovered by heating. This phenomenon has been recently called an ET-coupled spin transition (ETCST),[4] a general term describing both thermal and light-induced processes. Such properties were reported for the first time by Hashimoto and co-workers in $K_{0.2}Co_{1.4}[Fe(CN)_6]\cdot 6.9H_2O$.[5] Interestingly, in this seminal work, an opposite photomagnetic effect was also observed, as a partial decrease in the magnetization was obtained upon irradiation of the sample with blue light. The reverse effect was small (<6% variation of the magnetization), but further work showed that the magnetization of an Fe−Co PBA thin film could be almost fully erased by near-IR irradiation.[6] Such a photoreversal effect was also recently observed in the Fe−Mn PBA $Rb_{0.88}Mn[Fe(CN)_6]_{0.96}\cdot 0.5H_2O$.[7] In all of these cases, the physical properties were shown to be very dependent on the composition of the material, which itself is correlated to the (microscopic) structure.[7,8] Actually, the structure of PBAs looks simple at first glance (cyanide ligands bridging the metal ions in a cubic network), but a closer look reveals a more sophisticated description. Indeed, PBAs are often nonstoichiometric compounds that contain variable amounts of inserted alkali metal ions and $[M(CN)_6]^{n-}$ vacancies. Whereas powder or single-crystal X-ray diffraction (XRD) provides an averaged view of the structure, other techniques (e.g., X-ray absorption[8] and NMR spectroscopy[9]) have proven that several metal ion surroundings coexist, even in the stoichiometric derivatives. Consequently, the observed macroscopic behavior in the photomagnetic Fe−Co PBAs is the result of interactions between different {Fe−CN−Co} units, so rationalizing the physical properties is a difficult task that often requires the combined use of sophisticated physical measurements.[10] In this context, the search for discrete cyanide-based Fe−Co model complexes has lately attracted strong interest.[11] Several research teams have used self-assembly of stable preformed building blocks to design molecular photomagnetic systems, including square model complexes.[12] In contrast with the three-dimensional PBAs, the electronic properties of the Fe−Co pairs here can be finely adjusted by controlling the coordination sphere of the metal ions. Astonishingly, although the number of photomagnetic Fe−Co molecular systems is increasing, no bidirectional effect has been reported to date. Herein we demonstrate that repeatable on/off photoswitching of the magnetization can be observed in a discrete Fe−Co system (Chart 1) by using magnetic measurements on powder and single-crystal XRD experiments under continuous irradiation.

In this study, we selected as the photomagnetic molecule the $\{Fe_2Co_2\}$ square compound $\{[Fe\{B(pz)_4\}(CN)_3]_2[Co(bik)_2]_2\}(ClO_4)_2\cdot 3H_2O$ (**1**) [$B(pz)_4$ = tetrapyrazolylborate, bik = bis(1-methylimidazol-2-yl)ketone]. This complex is known to exhibit efficient dia → para conversion under white-light

Received: September 12, 2012
Published: January 15, 2013

   dx.doi.org/10.1021/ja3087467 | J. Am. Chem. Soc. 2013, 135, 1653−1656

Chart 1. Simplified View of Reversible Photoinduced ET in 1 and On/Off Switching of the Magnetic Properties

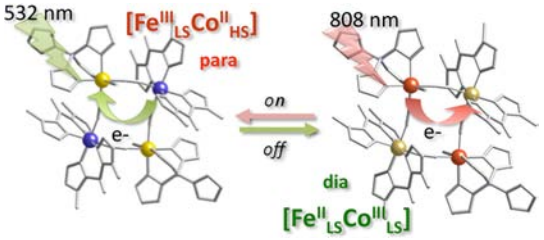

irradiation at 10 K. Its diamagnetic state can be recovered by heating it to 90 K.[12b] No photomagnetic effect can be observed above 60 K because the thermal relaxation is too fast. In the present study, we explored the photosensitivity of **1** at different wavelengths.

On-switching mode. Four different laser sources covering the visible range (405, 532, 635, and 808 nm) were used to irradiate **1** at 20 K. A significant photomagnetic effect was observed at each wavelength, but the increase in the $\chi_M T$ product (where χ_M is the molar magnetic susceptibility per Fe_2Co_2 unit) was greatest by far at 808 nm (Figure 1a). In all of these experiments, the

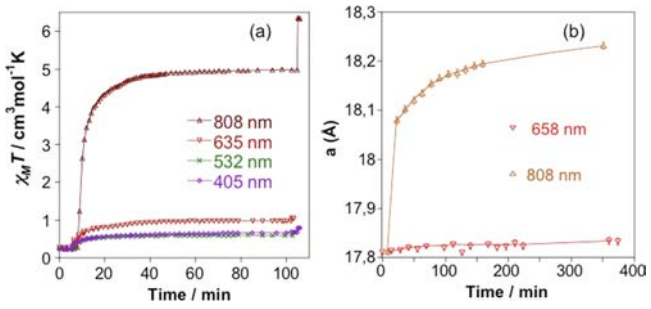

Figure 1. *On-switching mode.* (a) Plots of $\chi_M T$ vs time for **1** irradiated at 405, 532, 635, or 808 nm at a laser power of 5, 10, 12, or 6 mW/cm^2, respectively. (b) Variation of the *a* unit-cell parameter of **1** irradiated at 658 nm (70 mW/cm^2) or 808 nm (60 mW/cm^2). The last points near 400 min correspond to measurements done after complete data collections for structural refinement.

temperature was set to 20 K to minimize the heating of the sample caused by the laser irradiation. Nonetheless, this effect could not be completely avoided, even with moderate laser power, and resulted in a jump in $\chi_M T$ as the light was switched off. The effect was stronger for greater dia → para conversion. The persistence of the paramagnetic Fe^{III}–Co^{II} metastable state after the light was switched off was also checked [Figure S2 in the Supporting Information (SI)]. The $\chi_M T$ value used to evaluate the dia → para conversion rate was that measured in the dark, as the temperature of the sample was reliable and stable. In the case of irradiation at 808 nm, $\chi_M T$ reached ca. 6.5 cm^3 mol^{-1} K, which compares well to that measured in analogous $\{Fe^{III}_2Co^{II}_2\}$ model compounds,[13] indicating almost complete conversion of the diamagnetic Fe^{II}–Co^{III} pairs into paramagnetic Fe^{III}–Co^{II} pairs. Under this assumption, the rate of formation of paramagnetic pairs in **1** after irradiation at the other wavelengths was much lower, varying between 11 and 16%. The temperature dependence of the $\chi_M T$ product in the paramagnetic photoinduced state was recorded after it reached saturation (ca. 200 min at 808 nm; Figure S1). Complementary XRD studies were carried out at low temperatures under light irradiation to prove the photomagnetic effect on single crystals and to substantiate the nature of the photoinduced state. The crystal structure of **1** was first investigated at 80 or 15 K after quenching the sample in a nitrogen or helium flux. Comparison of the unit-cell parameters at 250,[12b] 80, and 15 K (orthorhombic space group *Pbcn*, $Z = 8$) showed that *b* first slightly increased and then decreased as *T* was lowered from 250 to 15 K, whereas *a* and *c* uniformly decreased (Table S1 in the SI). Selected average bond lengths and angles are reported in Table 1. Overall, the structure of the square motif

Table 1. Unit-Cell Parameters and Volumes, Average Metal-to-Ligand Bond Lengths, and Deformation of the First Coordination Sphere of Co for 1 under Different Experimental Conditions

	laser off		laser on, 15 K	
	80 K	15 K	808 nm ($\mathbf{1}^{808}$)	532 nm ($\mathbf{1}^{532}$)
a (Å)	17.8483(8)	17.688(4)	18.255(1)	17.952(1)
b (Å)	16.3064(6)	16.271(1)	15.9985(9)	16.133(1)
c (Å)	28.884(1)	28.886(1)	29.536(2)	29.016(2)
V (Å^3)	8406.6(6)	8307.7(9)	8626.3(7)	8403.6(9)
⟨Co–N⟩ (Å)	1.914(4)	1.919(3)	2.086(7)	1.950(8)
$\sum$ (deg)[a]	18(2)	20(2)	41(3)	19(3)
⟨Fe–N⟩ (Å)	1.991(4)	1.995(4)	1.974(6)	1.983(8)
⟨Fe–C⟩ (Å)	1.872(6)	1.874(4)	1.920(9)	1.88(1)

[a] $\sum = \sum_{i=1}^{12} |90 - \phi_i|$, where the ϕ_i are the N–Co–N bond angles.

did not show significant differences compared with that measured at higher temperatures:[12b] the bond lengths at the iron center match well with those previously observed for other Fe^{II}_{LS} complexes,[11] whereas the relatively short average Co–N bond length is typical of a Co^{III}_{LS} ion.[12,14]

The unit-cell parameters of a single crystal of **1** (300 μm × 300 μm × 200 μm) that was quenched at 15 K in a helium flux were measured during laser irradiation at 658 or 808 nm (Figures 1b and S3). Whereas the structural effects of the irradiation at 658 nm were very small (the increase in the cell volume, *V*, was <0.1%), irradiation at 808 nm induced a significant variation of the cell parameters: *a* and *c* continuously increased whereas *b* decreased (Figures 1b and S3). Overall, *V* increased by ca. 180 Å^3 (2.25% of the initial volume) after 160 min of irradiation (Figure S3). Crystallographic data were then collected during irradiation at 808 nm in order to identify the crystal structure of the photoinduced state, $\mathbf{1}^{808}$. The values of the *a* and *b* measured at the end of the XRD experiment were slightly different from those measured at the beginning, suggesting that the crystal conversion was not complete after 160 min of irradiation, but it was sufficient to study the nature of the photoinduced state (Figure S3). The space group of $\mathbf{1}^{808}$ was still *Pbcn* ($Z = 8$), but important changes in the coordination sphere of the Co ion occurred (Table 1, $\mathbf{1}^{808}$). The average ⟨Co–N⟩ bond length became 2.086(7) Å, which is close to that expected for a Co^{II}_{HS} ion,[8,13] suggesting almost complete spin-state conversion. Indeed, the Co–N bond length are expected to increase by ca. 0.18 Å when the LS d^6 configuration is transformed into the HS d^7 configuration, in agreement with the electron occupancy of the antibonding e_g^* orbital in the d^7 configuration.[8] In addition, the values of the N–Co–N angles in the coordination sphere of the HS Co ion departed more significantly from orthogonality than those measured in the LS state (Table 1). Although the Fe coordination sphere showed only smaller differences (Table 1), the change in the Fe charge is visible in the values of Fe–C bond distances. Whereas the Fe–C bond lengths were in the range 1.86–1.89 Å before irradiation, the average distance

dx.doi.org/10.1021/ja3087467 | J. Am. Chem. Soc. 2013, 135, 1653–1656

increased to >1.92 Å under 808 nm irradiation, evidencing the conversion of Fe^{II}_{LS} to Fe^{III}_{LS}.[12c] Thus, the crystal data match well with the occurrence of a light-induced ETCST (LIETCST) from an Fe^{II}_{LS}–Co^{III}_{LS} ion pair to an Fe^{III}_{LS}–Co^{II}_{HS} ion pair. This process was also accompanied by subtle changes in the geometry of the $\{Fe_2Co_2\}$ square motif. The Fe–Co intramolecular distances became significantly longer (increasing by ca. 0.2 Å), and the cyanide bridges were slightly more distorted on the Co side in the metastable paramagnetic state (Table S2). These intramolecular geometrical variations were also accompanied by modifications in the intermolecular interactions, with the short contacts between the square units, the water molecules and the perchlorate ions being modified (Figure S4 and Table S3).

Off-switching mode (reverse LIETCST). The photosensitivity of the photoinduced metastable paramagnetic state was then probed by measuring the evolution of $\chi_M T$ under laser irradiation at 405, 532, and 635 nm (Figure 2a). All of these wavelengths

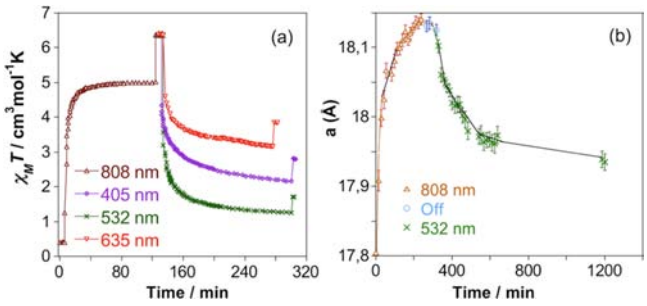

Figure 2. *Off-switching mode.* (a) Plot of $\chi_M T$ vs time for the metastable induced state irradiated at 405, 532, or 635 nm at a laser power of 5, 10, or 12 mW/cm^2, respectively. (b) Variation of the *a* unit-cell parameter of **1** upon successive laser irradiation at 808 nm (60 mW/cm^2) and 532 nm (85 mW/cm^2). The last points near 1200 min correspond to measurements done after complete data collections for structural refinement.

induced decreases in the magnetization, which can be ascribed to partial depopulation of the metastable state toward the diamagnetic ground state. The most efficient effect was observed at 532 nm, with $\chi_M T$ decreasing from ca. 6.4 to ca. 1.7 cm^3 mol^{-1} K after 200 min.[15] This variation corresponds to 73.5% recovery of the diamagnetic state.[16] The magnetization did not completely vanish for any of the laser sources used. This is consistent with the previous results observed in the on-switching mode, where all of the sources induced a noticeable increase in the magnetization. Indeed, it appears that the more efficient the source is in the on-switching mode, the less efficient it is in the off-switching mode. However, irradiation at a given wavelength did not yield the same $\chi_M T$ values in the on-switching and off-switching modes. For example, the 532 nm laser light induced a ca. 11% conversion toward the Fe^{III}_{LS}–Co^{II}_{HS} paramagnetic state in the on-switching mode, whereas it reduced the number of paramagnetic pairs to ca. 26.5% of the maximum value in the off-switching mode. A light penetration length smaller than the sample size as well as slower kinetics in the off-switching mode could account for these differences. The reversibility of the photomagnetic effect was also tested on a single crystal with roughly the same size as that used in the first experiment (300 μm × 200 μm × 200 μm). The variations of the crystallographic parameters (*a*, *b*, *c*, and *V*) upon successive irradiation at 808 and 532 nm are depicted in Figures 2b and S5. As in the first experiment, a steady state was obtained in the on-switching mode after ca. 300 min, and it persisted when the laser was turned off. Although the measured crystallographic parameters differed slightly from those obtained for the first crystal, their relative variations were very similar. For example, *V* increased by ca. 2% after 200 min, which is consistent with the increase in the Co–N bond lengths associated with the spin transition of the Co^{II} center. On the contrary, irradiation at 532 nm induced a significant decrease in *V* and variations in the cell parameters opposite to those observed under 808 nm irradiation (Figure 2b). XRD data were collected after irradiation of the crystal at 532 nm for 320 min, as the variation of the cell parameters as a function of time became very weak. Nonetheless, the cell parameters obtained after this collection were still slightly smaller than those measured before, indicating slow kinetics of the off-photoswitching under the present experimental conditions. The crystal structure of the resulting photoinduced state, $\mathbf{1}^{532}$ (*Pbcn*, *Z* = 8) exhibited bond lengths, angles, and intermolecular distances that were intermediate between those observed in **1** and $\mathbf{1}^{808}$, indicating partial recovery of the diamagnetic state. The average ⟨Co–N⟩ bond distance significantly decreased upon irradiation. By comparison of the measured distance [1.950(8) Å] with those expected for the LS state (~1.91 Å) and HS state (~2.09 Å), the recovery of the diamagnetic state was estimated to be 70–75%, which is comparable to the value from the magnetic measurement (Figure 2a). A tentative study of a smaller crystal (100 μm × 100 μm × 50 μm) showed an even higher reverse-LIETCST effect on the unit-cell parameters, thus evidencing the better match between the penetration length of 532 nm light and the crystal size (Figure S6). Unfortunately, the crystallinity did not remain sufficient for the corresponding average structure to be obtained. It should be noted that a loss of crystallinity upon both on and off photoswitching was observed for all of the checked samples, as manifested by a decrease in the intensities of the Bragg peaks at high θ angles (Table S2) and the consequent increase in the errors bars for both the unit-cell parameters and average bond lengths (Figures 1b, 2b, S3, S5, and S6 and Table 1). This prevented us from cycling the on/off photoswitching of single crystals.

Cycling. Finally, successive reversible photoinduced effects were investigated using a powdered sample by following the $\chi_M T$ value under cycles of successive irradiation at 808 and 532 nm for ca. 400–500 min. The plots of $\chi_M T$ versus time shown Figure 3

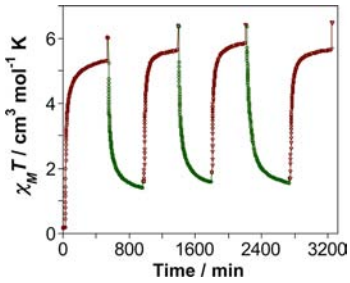

Figure 3. Plot of $\chi_M T$ vs time under cycles of successive irradiation at 808 nm (6 mW/cm^2) and 532 (10 mW/cm^2) nm at 20 K.

do not superimpose, but they do look similar. Interestingly, the first irradiation curve appears to be slightly below the following ones. This behavior was observed for several samples but remains unexplained at present. More importantly, the $\chi_M T$ values obtained after the on-switching and on-switching irradiations remained close to each other (ca. 1.6 and ca. 6.4 cm^3 mol^{-1} K). Therefore, the loss of crystallinity observed in the XRD

dx.doi.org/10.1021/ja3087467 | *J. Am. Chem. Soc.* 2013, 135, 1653–1656

experiments did not lead to a loss of the photomagnetic effect. A microscopic mechanism for bidirectional switching was first proposed by Kawamoto et al.[17] for photomagnetic Fe−Co PBAs. On the basis of *ab initio* quantum-chemical calculations, they postulated that the bidirectional effect would require the coexistence of two different Co surroundings, such as $\{Co(NC)_6\}$ or $\{Co(NC)_5(H_2O)\}$. The nonstoichiometric aspect of the PBA was said to play an essential role for the observation of the bidirectional photomagnetic effect: some Co chromophores would indeed be sensitive to red light, with the corresponding Fe^{II}_{LS}−Co^{III}_{LS} pairs being converted into Fe^{III}_{LS}−Co^{II}_{HS} ones, whereas other Co chromophores would be sensitive to near-IR irradiation, with the corresponding Fe^{III}_{LS}−Co^{II}_{HS} pairs being transformed into Fe^{II}_{LS}−Co^{III}_{LS} pairs. In both cases, the switching of the magnetic properties would be propagated from the sensitive site to its neighbors. In contrast, in the Fe−Co molecular model studied here, each Co ion strictly exhibits the same N_6 coordination sphere, and the photoswitching was observed starting from either the diamagnetic Fe^{II}−Co^{III} state or the metastable Fe^{III}−Co^{II} state. It is worth noticing that the efficient wavelengths in the on- and off-switching modes (808 and 532 nm, respectively) belong to the region where the $Fe^{II} \rightarrow Co^{III}$ and $Co^{II} \rightarrow Fe^{III}$ charge transfer (CT) bands are usually observed for similar square complexes,[12] in agreement with our optical study (Figure S9). The photomagnetic effect would involve initial ET followed by intersystem crossing of the excited state to the metastable state.[17] The reverse effect might also involve preliminary ligand-to-metal CT on the Fe center, as has been suggested for the Fe−Mn PBA derivative.[7] Finally, it is worth noting that although the $\{Fe_2Co_2\}$ square complexes remain at the present time the simplest model compounds for the more sophisticated Fe−Co PBAs, they still raise very difficult questions, such as whether the ET (i) occurs in both pairs simultaneously or (ii) preferentially occurs through one Fe−CN−Co edge or the perpendicular one. Our current efforts are being devoted to the study of the electronic states involved in the on/off photoswitching by using time-resolved experiments.

■ ASSOCIATED CONTENT

Supporting Information

Experimental section; additional figures and tables; CIFs for **1**, $\mathbf{1}^{808}$, and $\mathbf{1}^{532}$; and details of crystallographic and magnetic measurements. This material is available free of charge via the Internet at http://pubs.acs.org.

■ AUTHOR INFORMATION

Corresponding Author

marylise.buron@univ-rennes1.fr; rodrigue.lescouezec@upmc.fr

Notes

The authors declare no competing financial interest.

■ ACKNOWLEDGMENTS

This work was supported by the Ministère de l'Enseignement Supérieur et de la Recherche (MESR, France), the Erasmus Mundus Program (lot 13), the Agence Nationale de la Recherche (Project ANR-08-BLAN-0186-01 and ANR-09-BLAN-0212), Région Bretagne, the Ministerio Español de Ciencia e Innovación (CTQ 2010-15364), and Generalitat Valenciana (PROMETEO/2009/108 and ISIC2012/002).

■ REFERENCES

(1) (a) Feringa, B. L. *Molecular Switches*; Wiley-VCH: Weinheim, Germany, 2001. (b) Balzani, V.; Credi, A.; Venturi, M. *Molecular Devices and Machines: A Journey into the Nano World*; Wiley-VCH: Weinheim, Germany, 2003.

(2) Dei, A. *Angew. Chem., Int. Ed.* **2005**, *44*, 1160.

(3) Sato, O.; Einaga, Y.; Fujishima, A.; Hashimoto, K. *Inorg. Chem.* **1999**, *38*, 4405.

(4) Newton, G. R.; Nihei, M.; Oshio, H. *Eur. J. Inorg. Chem.* **2011**, 3031.

(5) Sato, O.; Iyoda, T.; Fujishima, A.; Hashimoto, K. *Science* **1996**, *272*, 704.

(6) Sato, O.; Einaga, Y.; Yidoa, T.; Fujishima, A.; Hashimoto, K. *J. Electrochem. Soc.* **1997**, *144*, L11.

(7) Tokoro, H.; Matsuda, T.; Nuida, T.; Motitomo, Y.; Ohoyama, K.; Dangui, E. D. L.; Boukheddaden, K.; Okhoshi, S.-I. *Chem. Mater.* **2008**, *20*, 423.

(8) (a) Cafun, J.-D.; Champion, G.; Arrio, M.-A.; Cartier dit Moulin, C.; Bleuzen, A. *J. Am. Chem. Soc.* **2010**, *132*, 11552. (b) Escax, V.; Champion, G.; Arrio, M.-A.; Zacchigna, M.; Cartier dit Moulin, C.; Bleuzen, A. *Angew. Chem., Int. Ed.* **2005**, *44*, 4798. (c) Bleuzen, A.; Escax, V.; Ferrier, A.; Villain, F.; Verdaguer, M.; Münsch, P.; Itié, J.-P. *Angew. Chem., Int. Ed.* **2004**, *43*, 3728.

(9) (a) Flambard, A.; Köhler, F. H.; Lescouëzec, R.; Revel, B. *Chem.—Eur. J.* **2011**, *17*, 11567. (b) Flambard, A.; Köhler, F. H.; Lescouëzec, R. *Angew Chem., Int. Ed.* **2009**, *48*, 1673.

(10) (a) Maurin, I.; Chernyshov, D.; Varret, F.; Bleuzen, A.; Tokoro, H.; Hashimoto, K.; Ohkoshi, S. I. *Phys. Rev. B.* **2009**, *79*, No. 064420. (b) Chong, C.; Itoi, M.; Boukheddaden, K.; Codjovi, E.; Rotaru, A.; Varret, F.; Frye, F. A.; Talham, D. R.; Maurin, I.; Chernyshov, D.; Castro, M. *Phys. Rev. B.* **2011**, *84*, No. 144102.

(11) (a) Li, D.; Clérac, R.; Roubeau, O.; Harté, E.; Mathonière, C.; Le Bris, R.; Holmes, S. M. *J. Am. Chem. Soc.* **2008**, *130*, 252. (b) Mitsumoto, K.; Oshiro, E.; Nishikawa, H.; Shiga, T.; Yamamura, Y.; Saito, K.; Oshio, H. *Chem.—Eur. J.* **2011**, *17*, 9612. (c) Funck, K. E.; Prosvirin, A. V.; Mathonière, C.; Clérac, R.; Dunbar, K. R. *Inorg. Chem.* **2011**, *50*, 2782. (d) Liu, T.; Dong, D.-P.; Kanegawa, S.; Kang, S.; Sato, O.; Shiota, Y.; Yoshizawa, K.; Hayami, S.; Wu, S.; He, C.; Duan, C. *Angew. Chem., Int. Ed.* **2012**, *51*, 4443. (e) Dong, D.-P.; Liu, T.; Kanegawa, S.; Kang, S.; Sato, O.; He, C.; Duan, C.-Y. *Angew. Chem., Int. Ed.* **2012**, *51*, 5119. (f) Nihei, M.; Okamoto, Y.; Sekine, Y.; Hoshino, N.; Shiga, T.; Liu, I. P.; Oshio, H. *Angew. Chem., Int. Ed.* **2012**, *51*, 6361.

(12) (a) Zhang, Y.; Li, D.; Clérac, R.; Kalisz, M.; Mathonière, C.; Holmes, S. M. *Angew. Chem., Int. Ed.* **2010**, *49*, 3652. (b) Mercurol, J.; Li, Y.; Pardo, E.; Risset, O.; Seuleiman, M.; Rousselière, H.; Lescouëzec, R.; Julve, M. *Chem. Commun.* **2010**, *46*, 8995. (c) Nihei, M.; Sekine, Y.; Suganami, N.; Nakazawa, K.; Nakao, A.; Nakao, H.; Murakami, Y.; Oshio, H. *J. Am. Chem. Soc.* **2011**, *133*, 3592. (d) Siretanu, D.; Li, D.; Buisson, L.; Bassani, D. M.; Holmes, S. M.; Mathonière, C.; Clérac, R. *Chem.—Eur. J.* **2011**, *17*, 11704.

(13) Pardo, E.; Verdaguer, M.; Herson, P.; Rousselière, H.; Cano, J.; Julve, M.; Lloret, F.; Lescouëzec, R. *Inorg. Chem.* **2011**, *50*, 6250.

(14) (a) Sharma, R. P.; Singh, A.; Brandao, P.; Felix, V.; Venugopalan, P. *J. Mol. Struct.* **2009**, *920*, 119. (b) Figgis, B. N.; Kucharski, E. S.; White, A. H. *Aust. J. Chem.* **1983**, *36*, 1563.

(15) An increase in $\chi_M T$ was observed in all of these experiments when the light source was switched off because of the temperature variation.

(16) This is in agreement with the magnetization value obtained at 2.0 K (Figure S7).

(17) Kawamoto, T.; Asai, Y.; Abe, S. *Phys. Rev. Lett.* **2001**, *86*, 348.